Effect of nonsinusoidal bias waveforms on ion energy distributions and fluorocarbon plasma etch selectivity

Ankur Agarwal
University of Illinois, Department of Chemical and Biomolecular Engineering, Urbana, Illinois 61801

Mark J. Kushner[a)]
Iowa State University, Department of Electrical and Computer Engineering, 104 Marston Hall, Ames, Iowa 50011-2151

(Received 12 May 2005; accepted 11 July 2005; published 16 August 2005)

The distributions of ion energies incident on the wafer significantly influence feature profiles and selectivity during plasma etching. Control of ion energies is typically obtained by varying the amplitude or frequency of a radio frequency sinusoidal bias voltage applied to the substrate. The resulting ion energy distribution (IED), though, is generally broad. Controlling the width and shape of the IED can potentially improve etch selectivity by distinguishing between threshold energies of surface processes. In this article, control of the IED was computationally investigated by applying a tailored, nonsinusoidal bias waveform to the substrate of an inductively coupled plasma. The waveform we investigated, a quasi-dc negative bias having a short positive pulse each cycle, produced a narrow IED whose width was controllable based on the length of the positive spike and frequency. We found that the selectivity between etching Si and SiO_2 in fluorocarbon plasmas could be controlled by adjusting the width and energy of the IED. Control of the energy of a narrow IED enables etching recipes that transition between speed and selectivity without change of gas mixture. © *2005 American Vacuum Society.* [DOI: 10.1116/1.2013318]

I. INTRODUCTION

The primary advantage of plasma-assisted etching of materials over wet etching for microelectronics fabrication is directional etching of small features due to energetic ion bombardment of the substrate.[1] The primary disadvantage is the difficulty of achieving selectivity in etching between two materials due to the dominance of physical as opposed to chemical processes.[2] Highly selective etching is important with respect to preventing excessive erosion of photoresist or underlying materials, and so allows over etching to compensate for nonuniformities of fluxes across the wafer.[3]

The characteristics of the plasma that influence etching or deposition profiles include the flux, and energy and angular distributions of reactant species onto the surface of the wafer. The magnitude of fluxes to the wafer are usually controlled by varying gas pressure, power deposition and feed gas mixture. For example, etching of silicon and silicon dioxide in high plasma-density tools has shown higher selectivity of SiO_2 over Si for feed gases with high carbon to fluorine atom ratios, such as C_2F_6 and C_4F_8,[4,5] or by the addition of H_2.[6,7] In selected cases, etch rates of SiO_2 have been shown to saturate on increasing power deposition in inductively coupled plasmas, presumably due to changes in the composition of the reactants.[8] In this regard, changes in the composition of the ion flux have been shown to not be the major influence on Si and SiO_2 etch rates.[9]

In fluorocarbon gas mixtures, the selectivity of SiO_2 over Si is based on the deposition of fluorocarbon films which regulate delivery of activation energy by ion bombardment to the substrate. Silicon surfaces, which are unreactive with the overlying CF_x polymer, typically support thicker polymer layers which then reduce the delivery of activation energy to the Si surface. SiO_2 surfaces, which react with the polymer, typically support thinner films which allow more efficient delivery of activation energy to the SiO_2 polymer interface. As such, etching of Si generally requires higher ion energies and biases in fluorocarbon plasmas to penetrate the thicker polymer layer than when etching SiO_2.

Selectivity can, in principle, be obtained by directly controlling the energy of ions which bombard the wafer surface. For example, if most ions bombarding the wafer have energies greater than the threshold energy of SiO_2 while being less than that of other materials such as Si, then, in principle, high selectivity can be obtained.[10] The differences in these threshold energies are typically only a few tens of eV, thereby requiring narrow ion energy distributions to obtain high selectivity. Secondary considerations in controlling the ion energies include the ion angular distribution to prevent aspect ratio dependent etch rates when the depth of the feature increases.[11]

Conventionally, control of the ion energy distribution (IED) at the substrate is obtained by varying the amplitude or frequency of a sinusoidal bias voltage waveform applied to the substrate. For a given voltage amplitude and mass of the ion, the width in energy of the IED can be controlled by varying the bias frequency[12] but this method suffers from two limitations. First, for a given frequency the width of the IED depends on the mass of the ion, being broader for lighter ions, and so maintaining a specified width of the IED is difficult with chemistries having a large variety of ions. Even

[a)]Author to whom correspondence should be addressed; electronic mail: mjk@iastate.edu

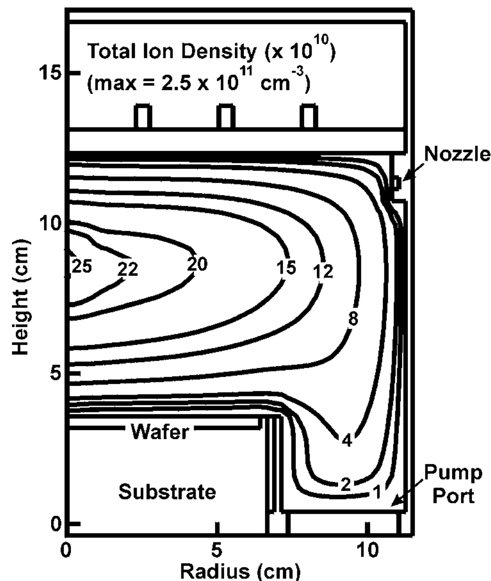

FIG. 1. Total ion density for the base case (Ar/c-C_4F_8, 500 W ICP Power, 15 mTorr, 100 sccm) and 200 V (peak-to-peak) substrate voltage. Contour levels shown are on a scale of 10^{10}.

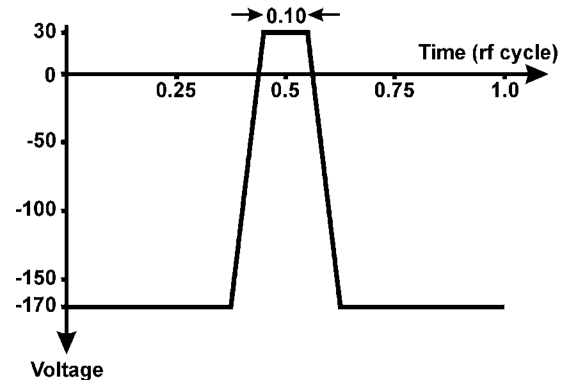

FIG. 2. Schematic of the tailored voltage bias waveform. The voltage waveform is $\alpha = 10\%$ based on the percent of the cycle with a constant positive voltage.

for high bias frequencies (>10s MHz) the IED tends to be wider for low mass ions in high plasma density reactors which have thin sheaths and short crossing times across the sheath. Second, at sufficiently high frequencies where IEDs for all ion masses are commensurate (>100s MHz), the rf wavelength may become comparable to the substrate dimensions. These nonuniformities in bias voltage across the substrate may produce unacceptable process nonuniformities.[13]

In the thin sheath limit, the energies and angular spread of ions at the wafer primarily depend on the instantaneous voltage drop when the ion enters the sheath. With a sinusoidal bias, the sheath voltage oscillates in time and so a broad IED results. This broad IED may include ions having high enough energy to breach the threshold energies for many materials, and so may not discriminate in etching those materials. Wang and Wendt[14] demonstrated that by using a tailored, nonsinusoidal bias voltage waveform, a narrow IED at the substrate can be achieved. This control is obtained by using a waveform which maintains the sheath voltage at a constant value for the majority of the rf cycle. Ions entering the sheath during this portion of the cycle strike the substrate with nearly a constant energy. Although there are issues associated with passing high frequency components through the finite impedance of the substrate and chuck, bias waveforms can be constructed to produce the desired sheath voltages.[14] Rauf computationally showed that sheath voltage above the wafer can be manipulated by the shape of the applied waveform, and so customize IEDs.[15]

In this article we report on a computational investigation of the shape of the IED and etching characteristics obtained with a tailored bias voltage waveform that was selected to achieve a narrow IED. The model system is an inductively coupled plasma (ICP) reactor operating in an Ar/c-C_4F_8 gas mixture etching SiO_2 over Si. The narrow IED was used to achieve high etch selectivity of SiO_2 over Si by positioning, in energy, the peak of the IED by either varying the shape of voltage waveform or the voltage amplitude. An etching recipe based on varying the amplitude of the tailored waveform was designed which results in a high etch selectivity at high rate without changing the gas chemistry.

The reactor and feature-scale models used in this investigation are described in Sec. II. Results from the investigation for controlling the IED and etch characteristics are discussed in Sec. III–V. Concluding remarks are in Sec. VI.

II. DESCRIPTION OF THE MODELS

Reactor scale properties and reactant fluxes to the substrate were obtained with the Hybrid Plasma Equipment Model (HPEM). The HPEM has been previously described and so will only be briefly discussed here.[16,17] The HPEM is a two-dimensional simulator which addresses equipment scale plasma chemistry and hydrodynamics, and consists of linked modules. Electromagnetic and magneto-static fields are calculated in the Electromagnetics Module. These fields are then used in the Electron Energy Transport Module to obtain electron impact source functions and transport coefficients. In the work presented here, the electron energy equation was utilized to obtain the average energy for the bulk electrons and a Monte Carlo simulation was used for transport of secondary electrons accelerated by the sheath. These results are then passed to the Fluid Kinetics Module, in which separate continuity, momentum and energy equations are solved for ions and neutral species. A drift diffusion formulation is used for electrons to enable an implicit solution of the Poisson's equation for the time varying electrostatic potential. Results from the Fluid Kinetics Module (densities and electrostatic fields) are then transferred to the other modules. This process is iterated until a converged solution is obtained.

The Plasma Chemistry Monte Carlo Module (PCMCM) in the HPEM produces the energy and angular distributions of neutrals and ions striking the surfaces in contact with the plasma. The PCMCM launches pseudoparticles representing ions and neutrals based on the electron impact source

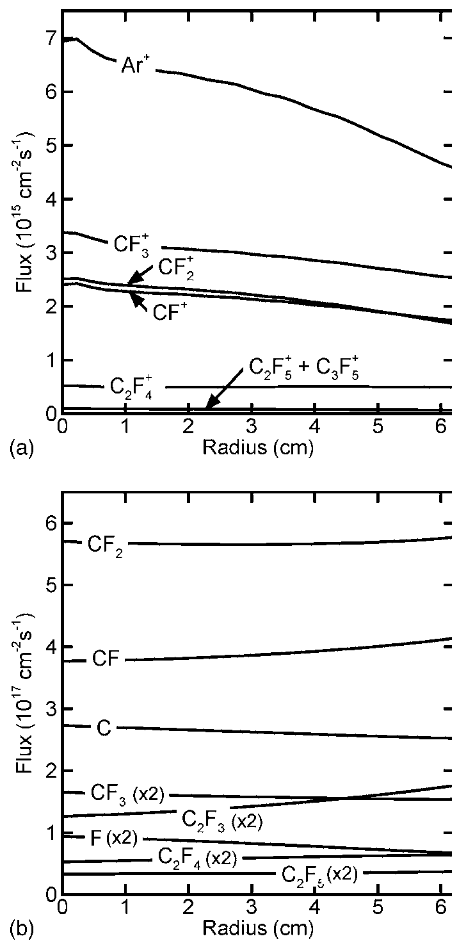

FIG. 3. Fluxes to the wafer as a function of radius for the base case conditions for Ar/c-C_4F_8 plasma. (a) Ion fluxes and (b) neutral fluxes. CF_2, CF, CF_3 are the dominant fluorine containing neutral radical fluxes. Ar^+, CF_3^+, CF_2^+ and CF^+ are the dominant ion fluxes.

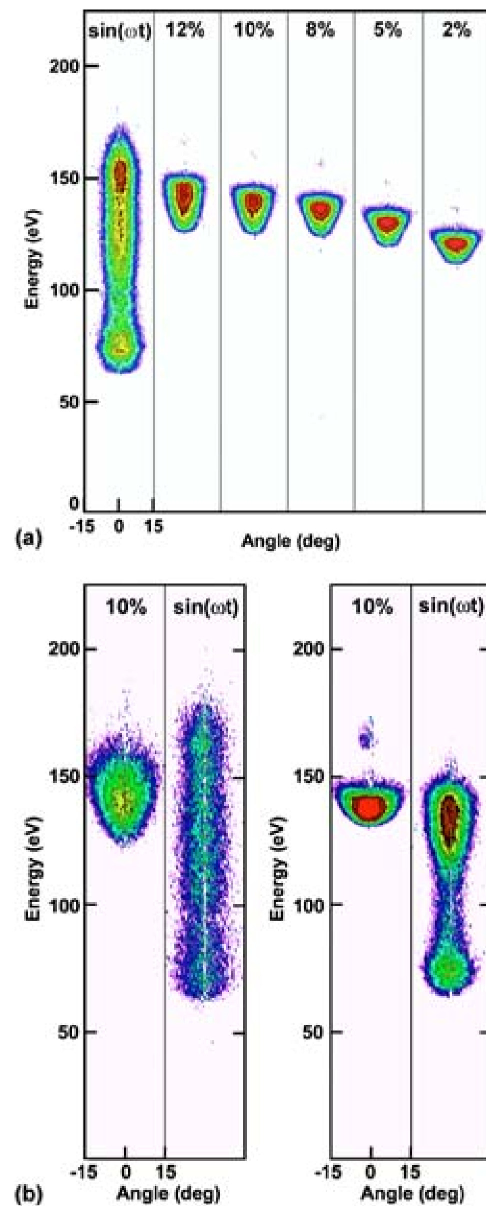

FIG. 4. Ion energy and angular distributions for different values of α (indicated as the percentage in each figure) compared to IEDs for a sinusoidal bias. (a) Ion energy and angular distributions for all ions. The tailored voltage waveform significantly narrows the spread in energy. (b) IEDs for F^+ (left) and $C_4F_7^+$ (right) ions for the $\alpha=10\%$ waveform and a sinusoidal waveform. The IEDs with the nonsinusoidal waveform are less sensitive to ion mass. IEDs are plotted as a 3 decade log scale.

functions and the time dependent electric fields obtained from the other modules of the HPEM. Using a Monte Carlo simulation, the PCMCM tracks the trajectories of the ions and neutrals while capturing their gas phase collisions and interactions with surfaces using the same reaction mechanism as in the HPEM. Statistics are collected on the energy and angle of pseudoparticles as they strike specified locations on the surfaces to produce time-averaged energy and angular distributions. The Monte Carlo Feature Profile Model (MCFPM) then uses these distributions at the wafer to predict etch profiles.

The two-dimensional MCFPM has been previously described and will only be briefly summarized here.[18,19] The fluxes of the reactant species and their energy and angular distributions from the HPEM are inputs to the MCFPM. The MCFPM resolves the surface (mask, photoresists, semiconductors) using a two-dimensional rectilinear mesh. Each cell in the mesh has a material identity. Pseudoparticles representing the incident plasma species are randomly selected from the energy and angular distributions obtained from the PCMCM and launched toward the surface. A generalized surface reaction mechanism controls the interaction between the gas-phase pseudoparticles and the computational mesh cells which represent the surface. The reaction mechanism is ultimately expressed as a probability array encompassing all possible reactions between the pseudoparticle plasma species and the surface species. When a pseudoparticle strikes a given material cell, a reaction is chosen based on these probability arrays using Monte Carlo techniques. Based on the selected reaction, the identities of the mesh cells are changed thereby representing deposition; or the cell is removed constituting an etch product. Gas-phase species evolving from these reactions are tracked as new gas-phase

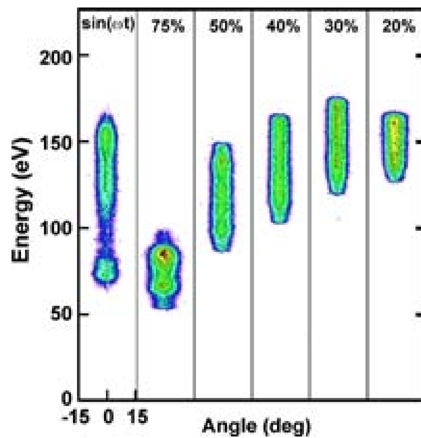

FIG. 5. Total ion energy and angular distributions, averaged over the wafer, for different values of α (indicated as the percentage in each figure) compared to the IED for a sinusoidal bias. The IEDs broaden and approach that for the sinusoidal bias as α approaches 50%. IEDs are plotted as a 2 decade log scale.

pseudoparticles. The mesh used to resolve our features consisted of square cells having dimensions of 1.5 nm or approximately ≈4 atomic spacings.

The specifics of the interaction of energetic particles with surface species are determined by their energy and angular distributions. The source of energetic particles is ions accelerated through the sheath, with energies of up to 100s eV and angular spreads ≈5–10° from the vertical. We assume that ions neutralize upon interaction with the surface and so do not distinguish between energetic ions and energetic neutrals. Energetic particles can either specularly of diffusively reflect from surfaces, with an energy loss which is larger for diffusive scattering and smaller for specular scattering.

III. INFLUENCE OF SHAPE OF RF BIAS WAVEFORM ON THE ION ENERGY DISTRIBUTION

The model system is an ICP reactor schematically shown in Fig. 1. Inductive power is supplied through a three-turn coil, 16 cm in diameter. The coil sits on a 2-cm-thick quartz window, which is 23 cm in diameter. The wafer is on a sub-

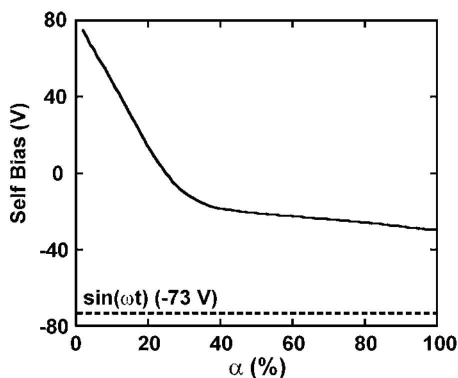

FIG. 6. Self-generated dc bias as a function of α. The self-generated dc bias voltage is −73 V for the sinusoidal waveform for the base case conditions. The bias, initially positive, becomes more negative as α increases and appears more symmetric.

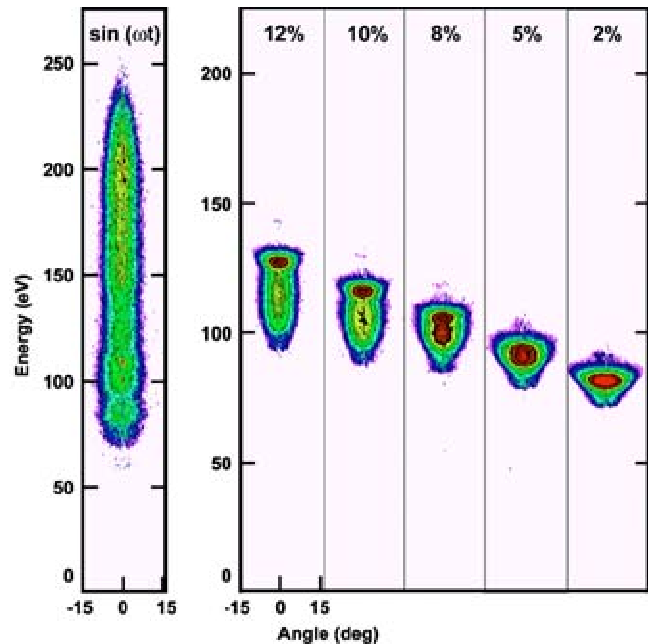

FIG. 7. Total ion energy and angular distributions, averaged over the wafer, for different values of α (indicated as the percentage in each figure) compared to the IED for a sinusoidal bias for 2 MHz excitation. IEDs are plotted as a 3 decade log scale.

strate, which can be independently biased, 7 cm below the quartz window. For the base case, a 15 mTorr Ar/c-C_4F_8 =75/25 gas mixture was used which enabled investigation of the effect of rf bias voltage on both high and low mass ions. For the base case, the flow rate was 100 sccm, the coil source was powered at 5 MHz and delivered a purely inductive power of 500 W. The shape and amplitude of the rf bias waveform will be varied at the electrode. The reaction mechanism for Ar/c-C_4F_8 mixtures was discussed and validated in Ref. 20.

The tailored nonsinusoidal bias voltage waveform used in this work is shown in Fig. 2. This voltage waveform consists of a quasi-dc negative bias to accelerate positive ions through the sheath with a narrow positive excursion to attract electrons and so balance the positive flux. The quasi-dc bias produces a nearly constant sheath potential as a function of time during the rf cycle which, if unperturbed by the positive voltage spike, would produce a narrow IED.[14] If the positive going excursion is of short enough duration, the heavy ions are unable to respond to the change in sheath potential and the perturbation to the narrow IED is minimal. The voltage waveforms have been characterized on the basis of the fraction of the time that the voltage is positive in one rf cycle, α. Based on this terminology the voltage waveform shown in Fig. 2 is an α=10% waveform.

The total positive ion density for the base case (α=10%, 200 V peak to peak) is shown in Fig. 1. Corresponding radical and ion fluxes to the wafer are shown in Fig. 3. The large electron density (≈10^{11} cm^{-3}) highly dissociates the c-C_4F_8 feedstock. As a result, the major fluorine containing radical fluxes are CF_2, CF, CF_3, and F, as observed experimentally

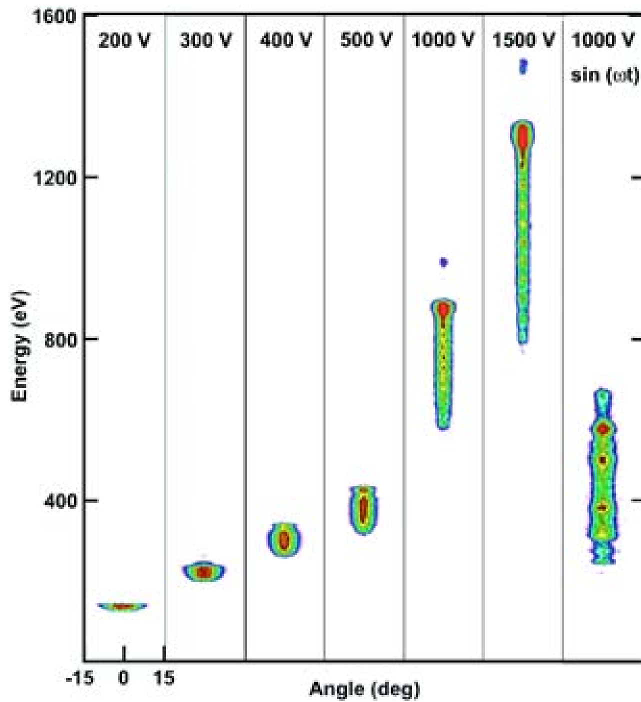

FIG. 8. Total ion and angular energy distributions, averaged over the wafer, for different peak-to-peak voltages for $\alpha=10\%$. The IEDs broaden with increasing voltage due to thickening of the sheath. IEDs are plotted as a 3 decade log scale.

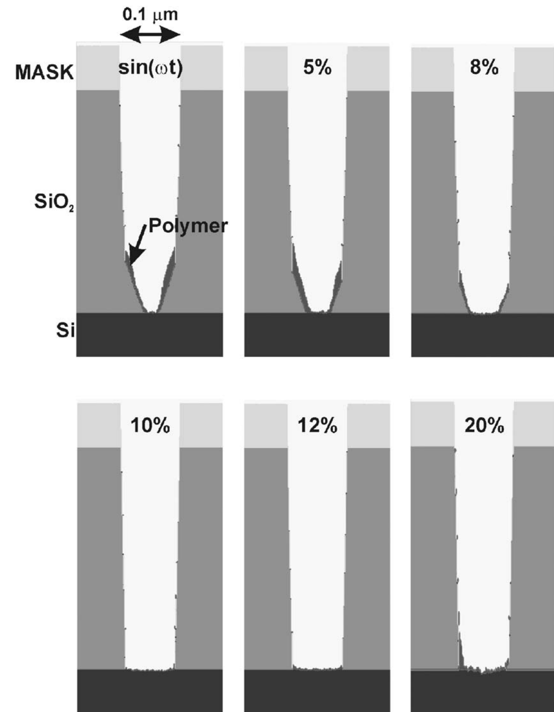

FIG. 9. Final etch profiles for different values of α for the base case conditions. Low α produces IEDs which result in etch-stop layers.

for comparable conditions.[21] The high degree of dissociation also results in the major ion fluxes consisting of Ar^+, CF_3^+, CF_2^+, and CF^+. The total ion density peaks at the center of the reactor, as do ion fluxes. This peaking is due, in part, to the accumulation of negative ions at the peak of the nearly quasi-dc plasma potential, and the need for a neutralizing positive ion flux. Lower F atom and ion fluxes may result in a thicker passivation layer near the edge of the wafer. In contrast, decreasing polymerizing fluxes may result in thinner polymer layer near the edges. The net result of the two opposing effects is that the etch rates near the edge of the wafer are slightly lower than at the center.

Time-averaged IEDs (sum of all ions) are shown in Fig. 4(a) for $\alpha=2\%$ through 12% waveforms and for a sinusoidal waveform (200 V peak to peak, 5 MHz). The sinusoidal voltage waveform produces the familiar broad IED which results from ions of different masses entering the sheath at random times during the rf cycle. The time required for the lighter ions (e.g., F^+, CF^+) to cross the sheath is commensurate with the rf period and so they arrive at the substrate with nearly the instantaneous sheath potential. The heavier ions (e.g., $C_2F_4^+$) may require many rf periods to cross the sheath, and so arrive with a narrower energy distribution centered on average sheath potential. The end result is a fairly broad IED, in this case extending for 85 eV.

The peak-to-peak voltage for the tailored waveforms is also 200 V at 5 MHz, divided between a −170 V quasi-dc portion and a positive 30 V spike. The tailored waveforms generally produce a narrower IED than the sinusoidal case in large part because the sheath voltage remains constant between the positive going spikes of the bias. The transit time across the sheath for the lighter ions is short compared to the pulse period, so the energy of each ion depends on the instantaneous potential drop when it enters the sheath.[14] As with the sinusoidal bias, the heavier ions may require many rf cycles to cross the sheath, and so arrive at the substrate with an energy more akin to the average sheath potential. If the positive going voltage spike is of sufficiently short duration, the cycle averaged sheath potential does not vary significantly from the quasi-dc sheath potential during the negative voltage portion of the cycle, and so the IED is not significantly broadened. As α increases, the IED broadens since the sheath potential is on the average less negative for a larger fraction of the rf cycle. Note, however, that even for small α there is an intrinsic width to the IED. This width results, in part, from ions arriving at the edge of the sheath with a distribution of energies depending upon the value of the plasma potential at the location of their last collision. This spread in energy could be as large as a few times the presheath voltage (10 or 20 eV).

Based on these arguments, the IED with the tailored waveform should be less sensitive to ion mass than with a sinusoidal bias. The sensitivity to mass of the IED using the tailored waveform is demonstrated by the results shown in Fig. 4(b). IEDs are shown for F^+ (light) and $C_4F_7^+$ (heavy) ions for the tailored $\alpha=10\%$ and sinusoidal waveforms. The lighter ion has a broader IED which has a different shape from that of the heavier ion with the sinusoidal waveform. Using the tailored waveform, the IED for the lighter does

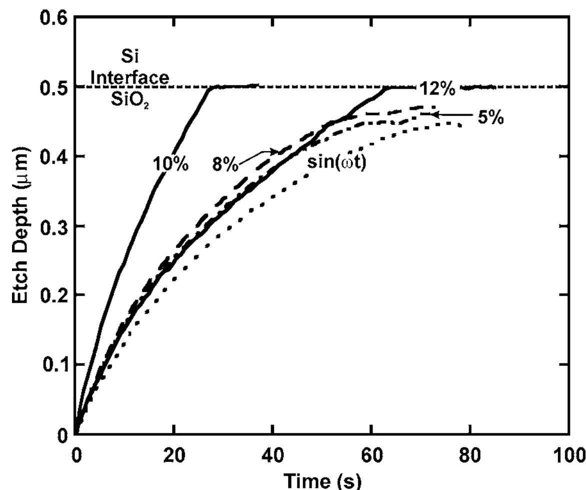

FIG. 10. Average etch depth as a function of time for different values of α. The etch rate increases with increasing α up to 10%. Above this value polymerizing reactions begin to dominate.

gain a small amount of breadth compared to the heavier ion, though the broadening is still a small fraction of the average energy

Time-averaged IEDs for all ions are shown in Fig. 5 for $\alpha=20\%$ through 75% waveforms (200 V peak to peak), and for a sinusoidal waveform. As the duration of the positive portion of the pulse increases, the IEDs broaden in energy and approach forms similar to that of sinusoidal IED. When the waveform exceeds $\alpha=50\%$, the waveform changes from being dominantly cathodic to being dominantly anodic, producing a thinner, lower voltage sheath. The bias begins to appear more like a positive dc bias than an rf bias. As a result, a narrower IED is again obtained, albeit with its average energy being lower.

The average applied voltage for the sinusoidal waveform is zero and, for this geometry, the resulting dc self-bias produced by the plasma is negative. The magnitude of this dc bias then adds to the energy of positive ions accelerated down the sheath. The time-averaged voltage for the nonsinusoidal waveform used here is negative. As a consequence, even in the absences of asymmetries in the reactor, the self-generated dc bias will be positive. The self-bias with the tailored waveform decreases towards negative values as the waveform becomes more symmetric and α approaches 50%, as shown in Fig. 6. For example, the dc bias for $\alpha=2\%$ is 75 V, decreasing to −21 V for $\alpha=50\%$. The increasing average ion energy as α increases, shown in Fig. 4(a), is due in part to this decrease in dc bias towards more negative values. The tailored waveform for $\alpha=40\%$ is essentially symmetric. As a result, the dc bias for that waveform should, in principle, differ from the dc bias for a sinusoidal waveform by 70 V, the offset voltage. The dc bias is, however, more negative than this expectation. The reason is that the $\alpha=40\%$ waveform has significantly higher harmonic content than the sine wave. These higher harmonics increase the displacement portion of the current, producing a more asymmetric collection of current.

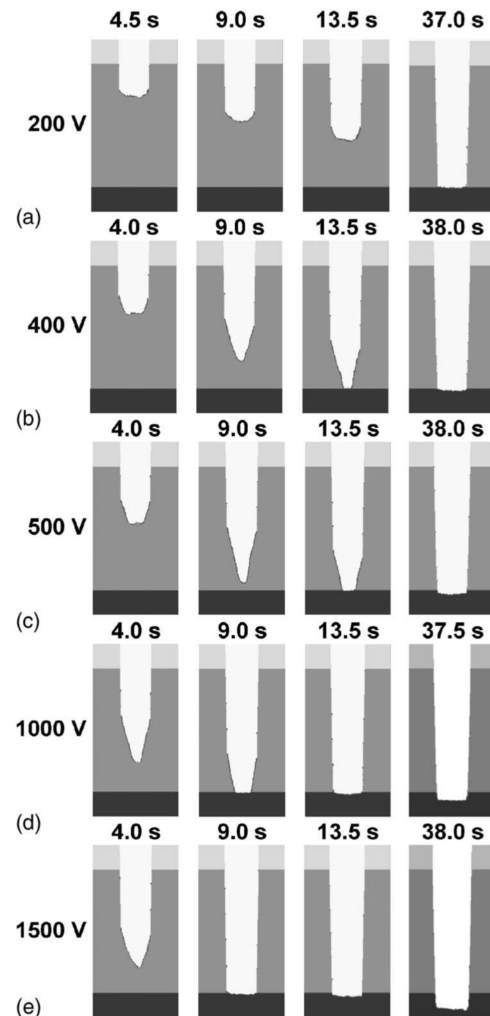

FIG. 11. Etch profiles at various times for different peak-to-peak voltages for $\alpha=10\%$ (a) 200 V, (b) 400 V, (c) 500 V, (d) 1000 V, (e) 1500 V.

To obtain a high etch selectivity, the width of the IED should be narrow enough so that the energies of the majority of ions striking the wafer fall between the threshold energies for etching the materials of interest. With the tailored waveform, this requirement can be met by varying the voltage amplitude, frequency or α. For example, time-averaged IEDs for the sum of all ions are shown in Fig. 7 for $\alpha=2\%$ through 12% waveforms and a sinusoidal waveform at a repetition frequency of 2 MHz. As is the case for 5 MHz (see Fig. 4), the IEDs for the tailored waveform are considerably narrower than for the corresponding sine wave bias. The IEDs at the lower frequency are controllably broader than at 5 MHz, affording some ability to tune to the IEDs.

Time-averaged IEDs for all ions are shown in Fig. 8 for $\alpha=10\%$ for different peak-to-peak voltages. The positive voltage excursion is 15% of the peak-to-peak voltage for all cases. As expected, the maximum and average energies of the tailored IEDs increase on increasing the peak-to-peak amplitude. In spite of keeping the ramp-up and ramp-down times constant, the IEDs tend to broaden in energy with increasing voltage. This broadening is due, in part, to the thick-

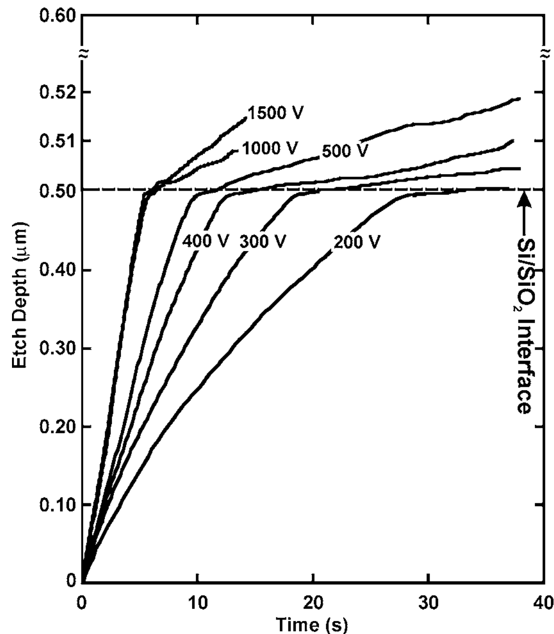

FIG. 12. Average etch depth as a function of time for different peak-to-peak voltages for α=10%. The etch rate increases as the voltage is increased but the selectivity decreases.

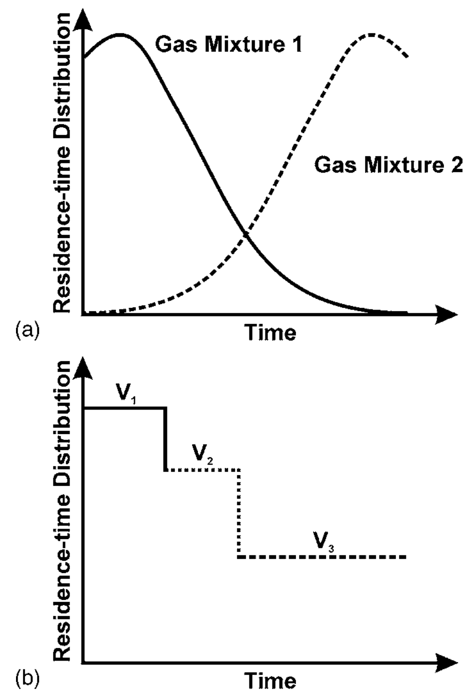

FIG. 13. Conceptual designs for main etch and over etch. (a) Recipe based on change of gas mixture. (b) Recipe based on change in voltage amplitude.

ening of the sheath at higher voltages which then requires longer transit times across the sheath. The residence time of some ions in the sheath therefore statistically overlaps with that portion of the cycle that the sheath potential is less negative, thereby extending the IED to lower energies. At the highest voltages this thickening results in the sheath becoming mildly collisional. The IEDs at higher voltages are, however, still narrow in energy when compared to the sinusoidal voltage waveform with the same peak-to-peak voltage. The angular width of the IEDs does narrow, however, monotonically as the bias voltage increases. There is also evidence of there being electrostatic waves that are launched into the plasma at higher biases by the impulsive, nearly step function change in substrate potential. This is particularly the case at higher voltages. These waves modulate the bulk plasma potential and are partly responsible for the modulation in the IED at energies below the peak.

IV. SILICON AND SILICON DIOXIDE ETCHING

Most ion-assisted etching or deposition processes have thresholds or energy dependent reactions that are sensitive to the distribution of ion energies. Control over the IED therefore has important implications with respect to selectivity. For example, if the width of the IED can be made narrower than the difference in threshold energies of two materials, and can be positioned so as to discriminate between their threshold energies, the resulting selectivity could in principle be infinite. A broad IED as might be obtained with a sinusoidal waveform may not allow for such discrimination.

Final predicted etch profiles for SiO_2 over Si are shown in Fig. 9 for a sine wave and tailored waveforms having α =5% through 20%. The IEDs for these cases are shown in Figs. 4(a) and 5. Polymer formation is promoted by low-energy ion bombardment, whereas the etch process and polymer removal are initiated by high-energy ion bombardment. Polymer is necessary for chemical sputtering of SiO_2 in fluorocarbon plasmas as the carbon in the polymer aids in removal of oxygen in the SiO_2. Lack of polymer can actually reduce the etch rate even at high ion energies by removing the reaction precursor. Selectivity of etching SiO_2 over Si is enabled by the low rate of reaction of Si with the polymer, which results in there being a thicker polymer layer on Si. A thicker polymer layer impedes the delivery of activation energy to the polymer-Si (or SiO_2) interface, thereby slowing or stopping the etch. For the waveforms having smaller values of α, the ions are low enough in energy that the polymerization reactions dominate over etching, and an etch stop occurs. This occurs deep into the trench as ion energies are degraded after reflection off of sidewalls. Upon increasing α, the ion energies increase and angular distributions narrow. As a result, there is less polymerization and less sidewall scattering. The feature is cleared while the IEDs are able to discriminate well between the threshold energies of SiO_2 and Si. The end result is high selectivity.

The average etch depth across the feature as a function of time is shown in Fig. 10 for different values of α. The etch rates have been scaled to match the reported experimental etch rates obtained for a sinusoidal waveform with a peak-to-peak voltage of 200 V.[20] The aspect ratio dependent etching (ARDE) is severe for low values of α as indicated by the progressively lower etch rate (slope of the line) with depth. There are increasing amounts of polymerization eventually leading to etch stops. This is also the case for the sinusoidal bias that has a larger proportion of low-energy ions. The etch

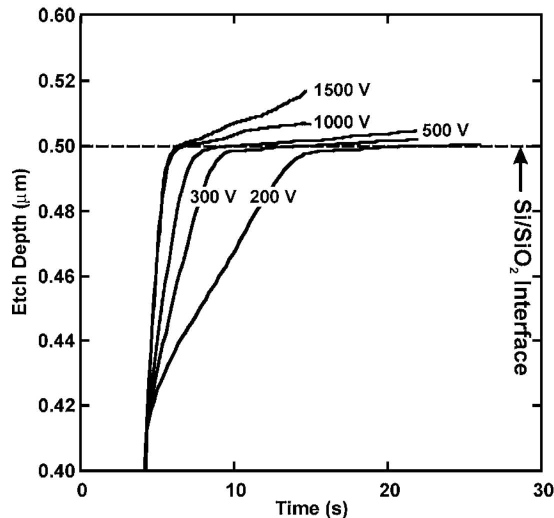

FIG. 14. Average etch depth as a function of time for different peak-to-peak voltages for $\alpha=10\%$. The voltage amplitude is changed at 4.5 s from 1500 V to lower voltages for the over-etch step.

rates increase with there being less ARDE as the positive portion of a cycle is increased (increasing α). The maximum etch rate is obtained with the $\alpha=10\%$ waveform with there also being good selectivity. However, as we approach the sinusoidal waveforms ($\alpha > 10\% - 20\%$) the etch rates begin to decrease again. As the IEDs broaden, the rate of polymerizing reactions increases and so the etch progresses more slowly.

Etch profiles at various times are shown in Fig. 11, for the tailored waveform ($\alpha=10\%$) for peak-to-peak voltages of 200 through 1500 V. Average etch depths as a function of time are shown in Fig. 12. As the peak-to-peak voltage is increased the ions have a higher energy on average and the etch proceeds more rapidly while there is less net polymer deposition. As a result the IEDs fail to discriminate between SiO_2 and Si at the higher biases and there is considerable overetching into the underlying Si. Although the positioning of the peak of the IEDs allows for higher etch rates, the selectivity that is obtained is also lower.

V. ETCHING RECIPES

Etching of features for microelectronics devices is often a multi-step process.[22–24] In addition to initial steps that remove top layers such as antireflection coatings or native oxide (in the case of p-Si), etching of high aspect ratio features usually consists of at least two steps. The first step is the main etch which is usually performed at high biases with nonpolymerizing chemistries that produce a nonselective but rapid etch. The second step is the over etch which is commenced when the interface with the underlying material is approached. This step is performed at lower biases and with a highly polymerizing chemistry that aids in selectivity. Traditionally, the steps are differentiated by controlling gas flow parameters such as gas mixture, flow rate, and pressure in addition to bias voltage. If this strategy is used, the change of gas composition in the reactor requires a finite period of time. Since gas transport is diffusive at low pressures, there will be components of both gas mixtures (main etch and over etch) in the reactor at the same time [See Fig. 13(a)]. The remnants of the main etch gases in the reactor during the over-etch step could compromise the ability to obtain high selectivity. As a result, one is motivated to develop recipes that rely only on the change of electrical characteristics, which can be changed virtually instantaneously, while using the same gas mixture for the main etch and over-etch steps.

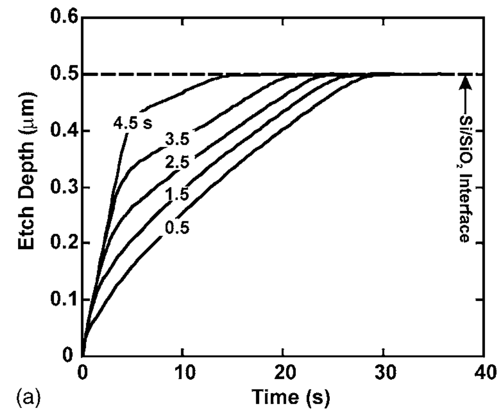

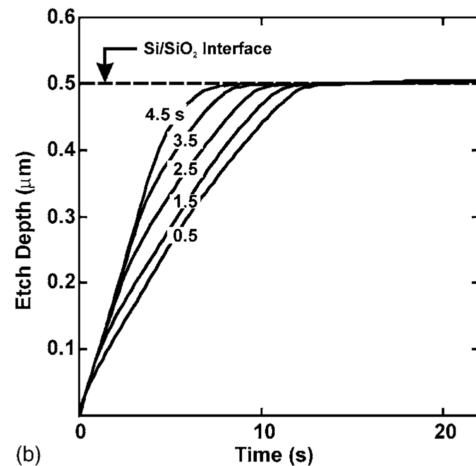

FIG. 15. Average etch depth as a function of time for a main etch voltage of 1500 V followed by a lower voltage for over etch at the indicated times. (a) 200 V and (b) 500 V.

To accomplish these goals, we used the tailored voltage bias waveform and made use of the fact that the energy of the peak of the IEDs can be positioned by varying voltage amplitudes. The bias voltage as a function of time is conceptually shown in Fig. 13(b). As the etch progresses from etch to over etch, the bias voltage is either sharply or gradually reduced so that the etch transitions from being rapid but nonselective to being selective but slower. If we regulate the peak of the IEDs to be such that it is able to distinguish between the thresholds of SiO_2 and Si then, in principle, infinite selectivity can be obtained while having a rapid etch.

Etch recipes were investigated for $\alpha=10\%$ waveforms where the main etch step is performed with a peak-to-peak potential of 1500 V and the over-etch step is performed with a lower voltage. The average etch depth across the feature as

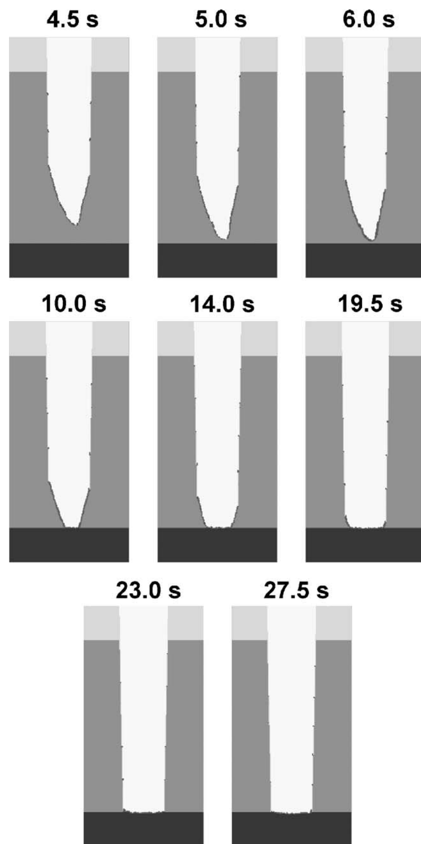

FIG. 16. Etch profiles for a main etch of 1500 V up to 5 s, followed by an over etch of 200 V. The time for changing the voltage to the lower, more selective value is determined by the taper obtained during the main etch.

a function of time is shown in Fig. 14 when the voltage is changed at $t=4.5$ s. The etch proceeds rapidly through the main etch step as polymerization is nominal (but adequate). In the absence of changing the voltage, the etch proceeds through the SiO_2-Si interface with poor selectivity. Upon lowering the peak-to-peak voltage at $t=4.5$ s, the etch rate slows while the selectivity improves. The end result is that a recipe having a large peak-to-peak voltage followed by a lower voltage can achieve the same selectivity but with higher net rate than using only the more selective lower voltage. For example, the 1500–300 V recipe clears the feature with high selectivity in ≈ 12 s whereas using a 300 V waveform alone requires ≈ 20 s.

The average etch depth across the feature as a function of time is shown in Fig. 15(a) for main etch step of 1500 V (peak to peak, $\alpha=10\%$) and an over-etch step of 200 V while changing the voltage at different times. In this case, the IEDs are narrow for the over-etch step which discriminates well between the thresholds of SiO_2 and Si, and a highly selective etch is obtained irrespective of the time of changing the voltage. Similar results are shown in Fig. 15(b) for an over-etch voltage of 500 V. High selectivity and high rates can be obtained by judicious choices of the main-etch and over-etch voltages, and the value of α. The nearly instantaneous change of etch rate afforded by the tailored bias enables precision control of the process. Timing the transition to the lower voltage to be as late as possible gains in rate while risking undesirable over etch at other locations on the wafer due to variations in the magnitude of the ion fluxes.

The profiles for a tailored waveform having $\alpha=10\%$, 1500 V (peak-to-peak) main etch and an over etch of 200 V (peak-to-peak) are shown in Fig. 16. The main etch step is run for 5 s and the over etch lasts for 22.5 s. The time at which the voltage is changed from 1500 to 200 V is determined by the lowest point of the taper. Had these conditions produced a flatter bottom to the trench, the main etch would have been able to proceed to a lower average depth prior to switching to the lower voltage. Small adjustments in the value of the α recoups some flatness of the profile bottom, and so enables the main etch to proceed closer to the interface before changing to the lower voltage.

VI. CONCLUDING REMARKS

The influence of the shape of the rf bias voltage waveform on ion energy distributions incident onto the wafer has been discussed based on results from a computational investigation using a reactor scale model coupled to a feature profile model. A nonsinusoidal waveform consisting of a quasi-dc negative bias with a narrow positive excursion was investigated in the context of fluorocarbon plasma etching of SiO_2 and Si. The tailored bias voltage waveform allows for precise control over the shape of the IED and the resulting distributions are less sensitive to the mass of the ions than using sinusoidal waveforms. This method for controlling the shape of the IED has potential for improving control of critical dimensions of etched features. This potential was demonstrated by proposing etching recipes based on rapidly changing the shape of the IED from one providing for a rapid but nonselective etch to one providing a slower but selective process.

ACKNOWLEDGMENTS

This work was supported by Semiconductor Research Corporation, National Science Foundation (CTS03-15303 and CTS05-20368) and Applied Materials Inc.

[1]M. Armacost, P. D. Hoh, R. Wise, W. Yan, J. J. Brown, J. H. Keller, G. A. Kaplita, S. D. Halle, K. P. Mller, M. D. Naeem, S. Srinivasan, H. Y. Ng, M. Gutsche, A. Gutmann, and B. Spuler, IBM J. Res. Dev. **43**, 39 (1999).
[2]E. Collard, C. Lejuene, J. P. Grandchamp, J. P. Gillers, and P. Scheiblin, Thin Solid Films **193**, 100 (1990).
[3]M. F. Dowmling, N. R. Rueger, G. S. Oehrlein, and J. M. Cook, J. Vac. Sci. Technol. B **16**, 1998 (1998).
[4]T. Fukasawa, A. Nakamura, H. Shindo, and Y. Horiike, Jpn. J. Appl. Phys., Part 1 **33**, 2139 (1994).
[5]J. A. O'Neil and J. Singh, J. Appl. Phys. **77**, 497 (1995).
[6]H.-H. Doh, J.-H. Jim, K.-W. Whang, and S.-H. Lee, J. Vac. Sci. Technol. A **14**, 1088 (1996).
[7]M. Haverlag, G. M. W. Kroesen, C. J. H. de Zeeuw, Y. Creyghton, T. JH. J. Bisschops, and F. J. de Hood, J. Vac. Sci. Technol. B **7**, 529 (1989).
[8]G. S. Oehrlein, Y. Zhang, D. Vender, and O. Joubert, J. Vac. Sci. Technol. A **12**, 333 (1994).
[9]K. H. R. Kirmse, A. E. Wendt, G. S. Oehrlein, and Y. Zhang, J. Vac. Sci. Technol. A **12**, 1287 (1994).
[10]S.-B. Wang and A. E. Wendt, J. Appl. Phys. **88**, 643 (2000).
[11]O. Joubert, G. S. Oehrlein, and Y. Zhang, J. Vac. Sci. Technol. A **12**, 658 (1994).

[12]W. M. Holber and J. Forster, J. Vac. Sci. Technol. A **8**, 3720 (1990).
[13]J. E. Stevens, M. J. Sowa, and J. L. Cecchi, J. Vac. Sci. Technol. A **14**, 129 (1996).
[14]S.-B. Wang and A. E. Wendt, J. Vac. Sci. Technol. A **19**, 2425 (2001).
[15]S. Rauf, J. Appl. Phys. **87**, 7647 (2000).
[16]R. L. Kinder and M. J. Kushner, J. Appl. Phys. **90**, 3699 (2001).
[17]R. L. Kinder and M. J. Kushner, J. Vac. Sci. Technol. A **19**, 76 (2001).
[18]R. J. Hoekstra and M. J. Kushner, J. Vac. Sci. Technol. A **16**, 3274 (1998).
[19]D. Zhang and M. J. Kushner, J. Vac. Sci. Technol. A **19**, 524 (2001).
[20]X. Li, L. Ling, X. Hua, G. S. Oehrlein, Y. Wang, A. V. Vasenkov, and M. J. Kushner, J. Vac. Sci. Technol. A **22**, 500 (2004).
[21]H. Nakagawa, S. Morishita, S. Noda, M. Okigawa, M. Inoue, M. Sekine, and K. Ito, J. Vac. Sci. Technol. A **17**, 1514 (1999).
[22]C. Monget, D. Fuard, O. Joubert, and J. P. Panabiere, Microelectron. Eng. **46**, 349 (1999).
[23]M.-R. Lin, P. Fang, F. Heiler, R. Rakkhit, and L. Shen, IEEE Electron Device Lett. **15**, 25 (1994).
[24]H.-C. Cheng, W. Lin, T.-K. Kang, Y.-C. Perng, and B.-T. Dai, IEEE Electron Device Lett. **19**, 183 (1998).